# On the potential effects of entrained air in centrifuge static liquefaction studies

D. Reid
*Red Earth Engineering, Perth, Australia, david.reid@redearthengineering.com.au*

R. Fanni
*WSP, Perth, Australia, riccardo.fanni@wsp.com*

N. Pereira
*Red Earth Engineering, Perth, Australia, Nicolas.Pereira@redearthengineering.com.au*

A. Fourie, V. Kunasegaram, F. Urbina

*The University of Western Australia, Perth, Australia, andy.fourie@uwa.edu.au, vijayakanthan.kunasegaram@uwa.edu.au, felipe.urbinaespinosa@research.uwa.edu.au*

**ABSTRACT:** Recent tailings storage facility and water dam failures have placed increased focus on static liquefaction, driving revisions to standards and guidelines along with more research into the triggering mechanism. One avenue of research has been application of geotechnical centrifuges to the study of the static liquefaction potential of slopes of loose soils or tailings. Much of this research has involved the study of the constant shear drained (CSD) mechanism, produced through the raising of the water level within a slope. Further, most recent studies appear to use viscous fluid to achieve hydraulic similitude, often without de-airing the fluid. Given the relatively low pore pressures present in the areas of slopes with highest stress ratio (i.e. near the toe), and existing awareness of the effects of entrained air on contractive soil response of loose samples sheared at constant water content, further investigation of the effect of entrained air on static liquefaction triggering of a CSD stress path is warranted. The current study investigates the effect of entrained air on the mechanical response of centrifuge tests by examining two centrifuge experiments featuring the CSD stress path within slopes of sand that appear to have failed under a higher phreatic surface (and, thus, higher stress ratios) than would typically be expected from element tests on the same material and field-scale examples. The response of these models is then investigated by means of CSD triaxial tests carried out under flushing and back pressure conditions, showing promising agreement.

## 1 INTRODUCTION

Static liquefaction of loose soils and tailings represents one of the greatest georisks, owing to the significant flow distance and, typically, lack of obvious external warning prior to the failure. Several prominent failures of tailings storage facilities (TSFs) and water dams have increased focus on static liquefaction. This has led to, for example, significant increases in efforts to model TSFs numerically to assess their potential to undergo static liquefaction triggering. However, there are significant ongoing uncertainties with this process (e.g. Reid et al. 2021) that remain largely unresolved. For example, the uncertainty of assessing liquefaction risks can, in a way, be demonstrated by post-failure investigations of Feijao, where three different groups all come to very different conclusions as to the failure mechanism (Robertson et al. 2019, Arroyo and Gens 2021, Zhu et al. 2024).

The geotechnical beam centrifuge forms, in principle, an ideal means to gain data and insight of static liquefaction failures of model slopes. This could then reduce uncertainties in the numerical modelling of TSFs – which remain significant (Reid et al. 2021, Reid and Fourie 2024) However, in recent works examining this mechanism (Ng et al. 2023) pre-failure instability was not seen - that is, a drained Factor of Safety (FoS) of ~1.0 was required for failure to occur, consistent with inferred stress paths achieving in situ stress ratio ($\eta = q/p'$) at, or exceeding, the critical state friction ratio $M$. Such testing has been carried out using $\sqrt{N}$ or $N$ viscosity pore fluids, consistent with persuasive arguments for the need for such scaling in static liquefaction assessments (e.g. Zhang and Askarinejad 2020).

The results of centrifuge experiments apparently requiring drained FoS =1 to initiate failure appears contradictory to element tests on loose soils following a CSD stress path which consistently undergo instability at stress ratios ($\eta_{IL}$) far lower than $M$ (e.g. Sasitharan et al. 1993) and case history data (Olson et al. 2000). Further, current TSF-related slope stability guidance (e.g. ICOLD B194) is not consistent with the suggestion that an initial failure surface with drained FoS ~1 is a requisite for static liquefaction initiation. Rather, the potential for pre-failure instability and triggering seems taken for granted in current TSF engineering practice (e.g. Reid and Fanni 2024). Finally, some centrifuge test programs using de-aired pore fluid (Zhang and Askarinejad 2019) with viscosity of $\sqrt{N}$ have undergone failure at slope angles that would seem difficult to reconcile with a hypothesised requirement of drained FoS = 1.

To further examine the apparently inconsistent results between (i) some centrifuge model static liquefaction failure experiments with water or with Methocell solution to increase viscosity and (ii) field-scale observations and current TSF stability guidance, two geotechnical beam centrifuge experiments on sand exposed to a CSD stress path are examined. Element tests of the same soil on a CSD path and similar saturation conditions to the centrifuge model are combined with numerical assessment of the in situ stress state within the slopes to examine the relevant stress ratio.

# 2 BEAM CENTRIFUGE EXPERIMENTS

## 2.1 Materials

The beam centrifuge tests were carried out using Silica Fine Sand (SFS), a standard research sand at The University of Western Australia (UWA). This sand has been thoroughly characterised by several relevant studies (Reid et al. 2023a, Souza et al. 2024). In particular, CSD tests under below-slope stress conditions were carried out across a range of states in both a hollow cylinder torsional system (Fanni et al. 2022) and a load-controlled direct simple shear (Reid and Fourie 2019), both being directly relevant to the centrifuge program, and both showing unambiguous evidence of pre-failure instability in loose samples.

## 2.2 Methocell effects

Although available studies generally suggest negligible effect on mechanical properties when using Methocell solutions, these have to our knowledge not been focussed on loose samples undergoing static liquefaction. To provide a check on the potential effect of Methocell on $\eta_{IL}$, a loose, isotropically consolidated undrained triaxial test was carried out using the current state of practice for loose samples (oversized lubricated platens, end of test soil freezing). The sample was moist tamped (MT) in a loose condition, then flushed and back pressure saturated with Methocell at $\sqrt{N}$ viscosity, where $N$=50 as per the centrifuge experiments outlined subsequently. The result in terms of $\eta_{IL}$ is presented in Figure 1, compared to the results of Reid et al. (2024) on the same sand with water as the pore fluid. Indistinguishable results are seen, consistent with previous examinations of the effect of Methocell on sand. This suggests that use of Methocell solutions will not affect the outcomes of centrifuge experiments with SFS.

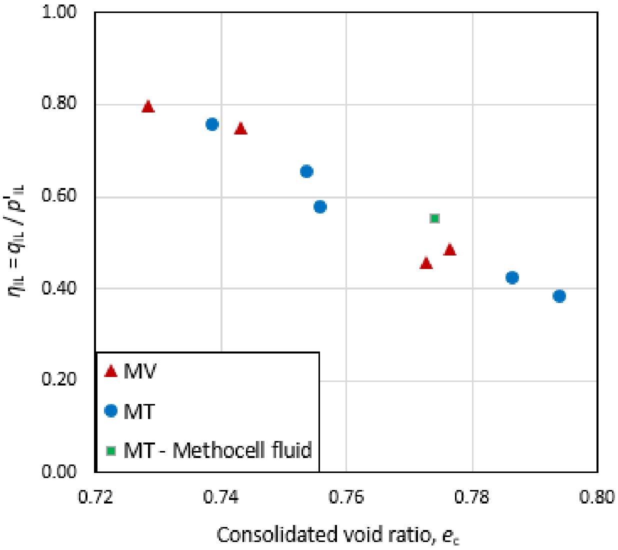


*Figure 1. Results of loose CIU triaxial test on MT specimen with $\sqrt{N}$ Methocell pore fluid, moist vibration (MV) and MT data after Reid et al. (2024).*

## 2.3 Equipment

The beam centrifuge tests were carried out in the 10m diameter C72 centrifuge at the National Geotechnical Centrifuge Facility (NGCF). The standard "strongbox" used in C72 is 1m square and 480mm deep. To facilitate slope preparation while allowing camera placement in line with the slope, a strongbox insert (with inner dimensions of 917 mm in length 400 mm breadth and 440 mm depth) was manufactured taking up approximately one half of the C72 strongbox. This insert included (i) total pressure cells (TPCs) embedded in the walls, (ii) pore pressure transducers (PPT) embedded in the floor and walls, (iii) a transparent acrylic face to enable imaging of the tests, (iv) a reservoir on the upstream side with filter media to allow a phreatic surface to be developed within the model, and (v) linear variable displacement transducers (LVDT) and laser displacement transducers (LDT) to monitor deformation of the system.

## 2.4 Test methods

SFS was moist tamped within the strongbox in 10 layers at an initial void ratio $e$ of 0.83 (Relative Density of -20%), an initial density that results in a loose state (refer Section 2.5). After placing the layers across the entire strongbox, the slope was then trimmed. The initial slopes cut for the two tests were 1V:2H and 1V:1.5H for water and Methocell tests, respectively. LVDTs and LDTs were then installed on the slope at the crest and targeting the lower portion of the slope as shown in Figure 2.

*Table 1. General features of the two tests outlined herein.*

| Test | Acc. (g) | Fluid | Prototype height (m) | Slope (V:H) |
|---|---|---|---|---|
| Test 1 | 50 | Water | 18 | 1:2 |
| Test 2 | 50 | $\sqrt{N}$ Methocell | 22 | 1:1.5 |

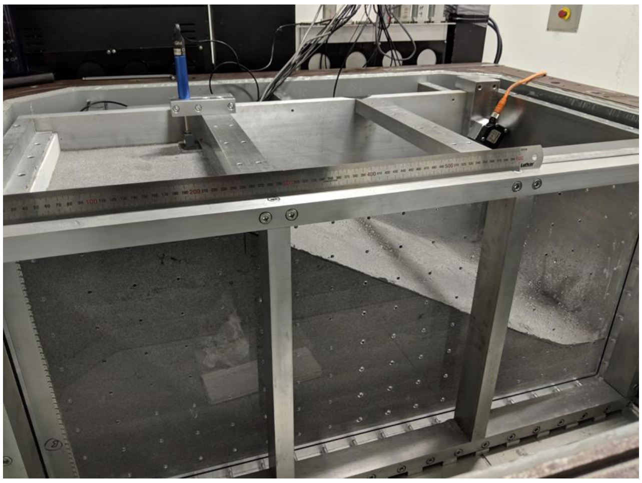

*Figure 2. Test 1 after preparation and placement of the slope insert within the C72 strongbox*

The centrifuge was spun to 50g and allowed to stabilise for 1 hr after reaching the target gravity. The TPCs were found to be generally unreliable with poor performance, with only two operational in Test 1. However, after stabilisation at 50g they provided an indication of $K_0$ = 0.47 – 0.55, consistent with expectations for SFS based on $K_0$ triaxial tests.

After stabilisation at 50g, water or viscous pore fluid was pumped into the upstream reservoir. The level in the reservoir was monitored by the piezometer at the base, to ensure it did not overtop and flow onto the crest of the SFS slope. This process was continued until slope failure was observed, as discussed subsequently.

## 2.5 Shear bias effects

A series of DSS tests were carried out to assess the effect of consolidation in moist conditions and the state achieved in portions of the model most relevant for stability (those saturated below the lower portion of the slope, having the highest $\eta$). In these DSS tests, consolidation was performed first, followed by saturation replicating the sequence applied in the centrifuge tests. (e.g. Reid et al. 2023b).

The stresses adopted in these tests were based on the outcomes of numerical models of the slope discussed subsequently, and involved (i) increasing vertical effective stress and horizontal shear stress while unsaturated (centrifuge ramping to 50g), (ii) inundation with water (first contact with phreatic surface advance) and (iii) reducing the vertical effective stress consistent with that which occurred in the model up to failure. The results of both models are summarised in Figure 3, indicating that zones below the slope that later became saturated would remain above the CSL, and thus susceptible – based on element tests – to instability at stress ratios lower than $M$.

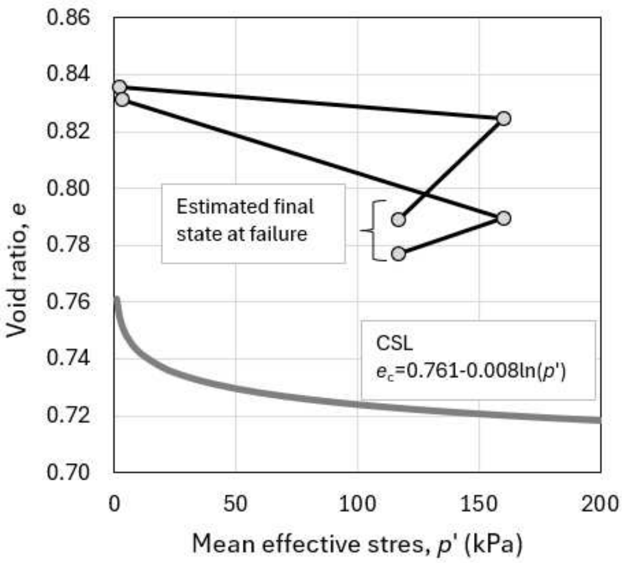


*Figure 3. Figure showing state diagram of two DSS tests with CSL, confirming their contractive state (mean effective stress, p', estimated assuming K0 = 0.5 during consolidation and at onset of failure)*

The results of the DSS tests carried out to represent the approximate stress path of the sand below the lower portions of the slope confirms that the material will be in a contractive state, and therefore informs expectations for the model behaviour that follows.

## 2.6 General centrifuge model behaviour

The models were successfully exposed to a rising phreatic surface without evidence of piping erosion from the slope. Both tests eventually exhibited a sudden failure with no obvious precursor in terms of preceding acceleration of displacement or pore pressure response (other than gradual buildup from the rising phreatic surface). All these features are consistent with expectations for static liquefaction failures under a rising phreatic surface.

Images of the slopes immediately before and after the commencement of significant movement are presented in Figure 4 and Figure 5 for Test 1 and 2, respectively. The cameras were capturing images at 10 frames per second (FPS) for Test 1 and 5 FPS for Test 2. The "before failure" images are the frame immediately preceding the commencement of significant movement. The areas where slope failure initiates are clear in both cases: Test 1 exhibited a relatively deep initial failure, with no evidence for an initial shallow slide either in the video perspective shown here or in a separate camera above the toe looking downwards; alternatively, Test 2 exhibited an initial shallow failure followed, one frame later, by a deeper mechanism – like the progression observed by Take and Beddoe (2014) and Coutinho et al. (2025) in their experiments.

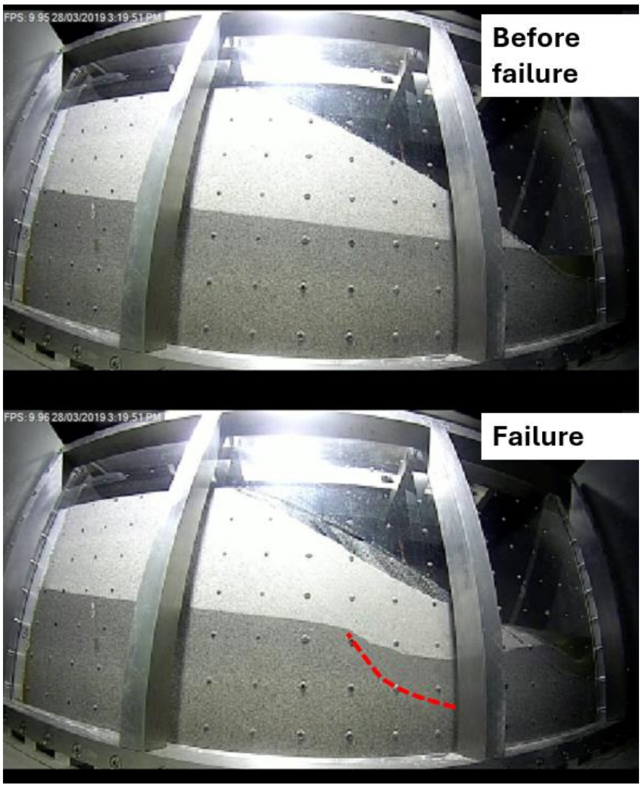


*Figure 4. Test 1, images showing frame (a) immediately before movement evident and (b) first indication of slope movement. Sequential frames shown, at 10 FPS capture rate.*

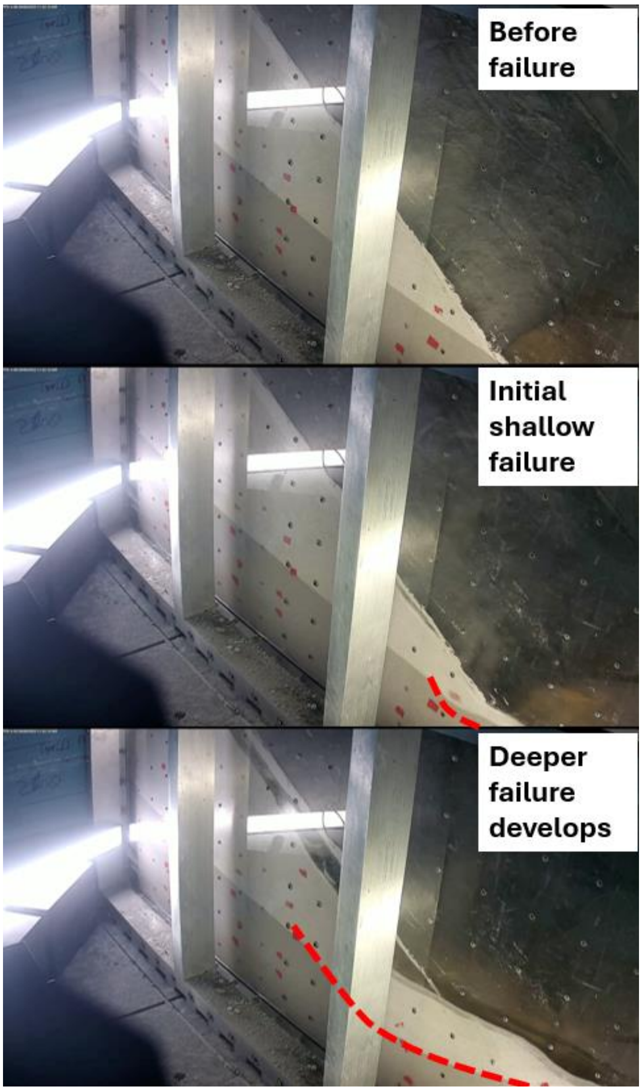


*Figure 5. Test 2, images showing frame (a) immediately before movement (b) first indication of slope movement, shallow failure and (c) mobilisation of deeper subsequent failure. Sequential frames shown, at 5 FPS capture rate.*

## 2.7 Limit equilibrium analyses

Initial analysis of the slopes at the time of failure was carried out using limit equilibrium (LE) methods with the commercial software code Slide2 v9. Above the phreatic surface, drained strength of $\phi$' = 31 degrees was adopted. A cohesion value of 5 kPa was assumed based on the unsaturated condition of the sand. The failures were investigated as follows:

- For Test 1, undrained $s_u/\sigma'_{vc}$ ratios were iteratively adjusted below the phreatic surface to produce a FoS of 1.0, for a failure surface drawn to match that observed in the video recordings. A value of $s_u/\sigma'_{vc} = 0.33$ produced a FoS of 1.0, with this value being significantly below the drained strength of the sand and therefore consistent with expectations for loose SFS. This model result is presented in Figure 6.

- For Test 2, the shallow initial failure was investigated. It was seen that a FoS near to unity could be produced simply with drained strengths for the sand (without cohesion below the phreatic surface) as shown in Figure 7. This being a result of the steeper slope in this model.

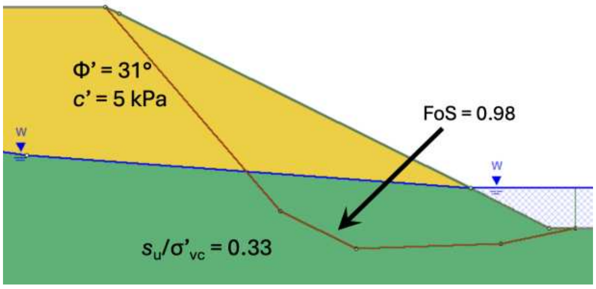


*Figure 6. LE model results for Test 1*

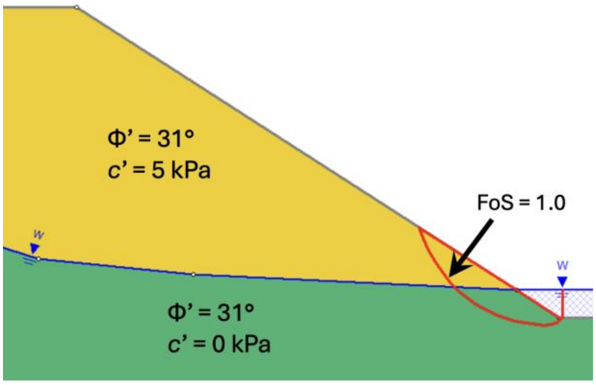


*Figure 7. LE model results for Test 2, shallow initial failure*

In general, Test 2's results are not of particular interest for the investigation of static liquefaction herein – the initial shallow failure being sufficiently explained by drained FoS ~1.0. This initial small failure triggering a subsequent deeper failure being consistent with previous data from Take and Beddoe (2014). Alternatively, Test 1's result indicates the potential that the slope behaviour involved pre-failure instability. This is investigated subsequently via numerical analyses.

## 2.8 Numerical analyses

To provide a more robust assessment of stress states in the area where failure initiated in Test 1, a two-dimensional model of the slope was developed using the finite difference code FLAC2D v9.5. Given the difficulty in reliably estimating stress states with advanced constitutive models the Mohr Coulomb model was used with assumed Poisson's ratio of 0.33, thus producing a $K_0$ of 0.5 (below level ground), consistent with experimental observations of SFS and the limited data available from the TPCs. It is emphasised that the only purpose of this model is to estimate stress conditions in the failure zone, not pre-failure deformations or any other aspect.

The results of the model when the phreatic surface reached the height at which failure occurred is presented in Figure  as $\eta/M$. The evolution of $M$ with intermediate principal stress ratio $b$ (used in the calculation of $M$) is based on the Mohr Coulomb failure criterion (i.e. it maintains a constant friction angle with $b$), consistent with the scaling adopted in the hollow cylinder torsional shear (HCTS) CSD tests on SFS carried out at a range of $b$ values (Fanni et al. 2022) and the unambiguous evidence for the requirement to scale $\eta_{IL}$ by $M$ (Fanni et al 2025) when synthesising such data. The numerical model results show high values (>0.95) of $\eta/M$ in a significant portion of the slope, which align reasonably well with the available visual evidence for failure initiation. The location where the failure surface emerged at the toe is unclear. However, the high values of $\eta/M$ just downstream of the toe in the numerical model are consistent with the assumption made in the LE model of the same slope (refer to previous Figure 6).

The crucial outcome of the slope interrogation provided by Figure , based on the testing of Fanni et al. (2022) on the sand under CSD stress path and predictions of the in situ state in the centrifuge (refer Section 2.5), is that element tests would suggest the slope should have failed far earlier than it did. Pre-failure instability is ubiquitous in all CSD testing on loose samples of the sand available. Importantly, all such tests are carried out with high quality saturation – that is, flushing with deaired water then back pressure saturation. This differs from the area with high $\eta/M$ in the slope examined here, which typically has pore pressures <50 kPa and which has only "just" become inundated – no ongoing flushing of multiple pore volumes of fluid has occurred in most areas as is typical in laboratory element tests (even prior to subsequent application of back pressure).

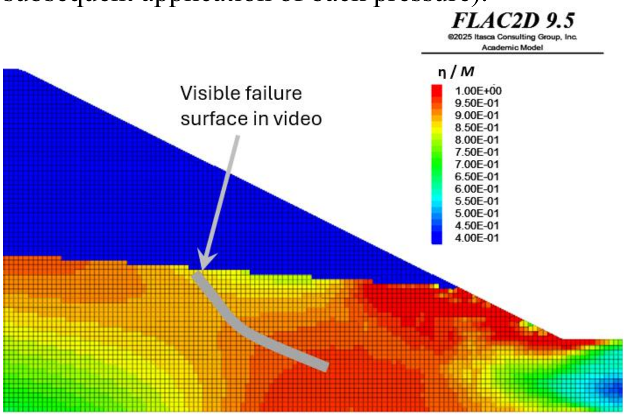


*Figure 8. Modelled distribution of η/M for Test 1, with phreatic conditions at time of slope failure*

A final note should be made regarding the stress conditions seen in Figure – in initial interrogations of the results, it was noted that the values of $\eta/M$ were higher than expected for a slope of this geometry. Examination of the same slope geometry, but with far wider plateau, toe extent, and depth showed lower values of $\eta/M$, and different stress distributions more generally. This highlights the effect of the constrained strongbox insert geometry and the importance of capturing these effects.

# 3 ADDITIONAL CSD EXPERIMENTS

## 3.1 Rationale

The results of the centrifuge tests and numerical model of Test 1 appeared to confirm that higher than expected stress ratios were required to trigger slope failure in a centrifuge CSD test than might be expected from full scale experience or element test response. To further investigate this, a series of CSD tests were carried out under conditions like those in areas of high stress ratio in the models. While constant water content tests (Wang et al. 2024, Urbina et al. 2025) have in the past shown the significant effect of entrained air on resulting instability, to our knowledge this has not been extended to CSD tests. This idea builds upon the discussion of Take et al. (2004) in the context of difficulties triggering static liquefaction failures in experimental simulations of slopes and the potential effect of saturation conditions.

## 3.2 Methods

CSD tests were carried out using SFS, in an electro-mechanic dynamic triaxial device able to aggressively maintain target deviator stress as displacement accelerates. Specimens were prepared using MT procedure in a loose condition. Three tests were carried out with the following saturation procedures:

1) Water was used as pore fluid, specimen saturated with conventional back pressure techniques, which achieved $B$ of 0.96.
2) Water was used as pore fluid, specimen was flushed with water until bubbles ceased emerging from the sample. Then back pressure was increased to 30 kPa.
3) $\sqrt{N}$ Methocell was flushed through sample in a similar manner to Test 2, then 30 kPa back pressure was applied.

The purpose of Tests 2 and 3 was to assess the response of samples that follow flushing/saturation conditions like that which would have occurred below the lower portion of the slope in the centrifuge tests. After the saturation procedures outlined, cell and deviator stresses were ramped to produce a condition of $q$ = 100 kPa and $p'$ = 133 kPa ($\sigma'_v$ =200, $\sigma'_h$ = 100). Then a CSD path was followed by increasing the pore pressure in the sample. Volume changes were monitored using cell volume.

## 3.3 Results

The results of the three tests are compared in Figure as a $p'$- $q$ and state diagram. The fully saturated test undergoes typical pre-failure instability, with rapid displacement and loss of control at $\eta$ ~0.83. Alternatively, the two tests with back pressure of 30 kPa (water or Methocell) exhibit strikingly different responses to the saturated test – significantly more contraction occurs, and the specimens remain stable until $M_{tc}$. This is consistent with unsaturated CSD testing (Skopek et al. 1994). It is further noted that both low back pressure samples had estimated $S_r$ of 80%– a value of $S_r$ similar to other studies with similar procedures.

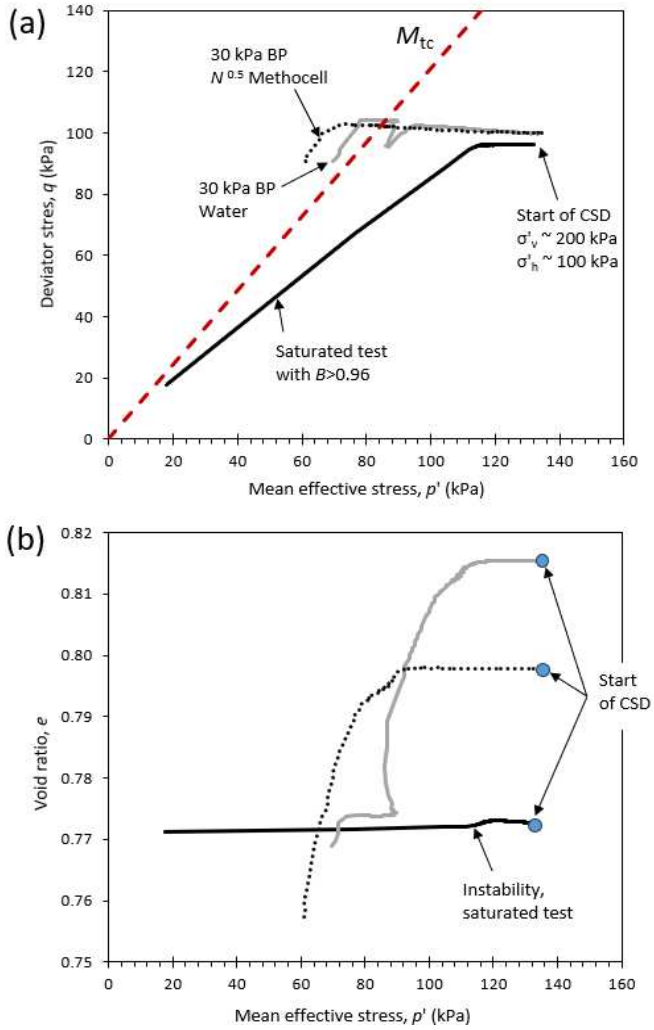


*Figure 9. Results of CSD tests with and without high quality saturation procedures: (a) p' – q plot, and (b) state diagram*

## 4 IMPLICATIONS AND DISCUSSION

The results of beam centrifuge experiments, both outlined herein and previous works highlight the difficulty of producing unambiguous examples of pre-failure instability in centrifuge slopes, particularly with a CSD stress path. A hypothesis put forward in this paper is that the process by which the centrifuge slopes under CSD stress paths are "saturated" – a rising phreatic surface of fluid that typically is not de-aired, is unlikely to produce full saturation, and thus are not as prone to pre-failure instability. The subsequent CSD experiments carried out to investigate this appear to provide support for this hypothesis.

Assuming, for argument's sake, that poor quality saturation plays a role in making pre-failure instability challenging in centrifuges then leads to broader questions. For example, there is widespread discussion in the groundwater literature about the "quasi saturated region", that is the area below the phreatic surface where significant entrained air is present (Faybishenko, 1995) – likely relevant to both the zones of the centrifuge tests outlined herein with high η and the CSD tests carried out to assess this region. Does this then mean that areas in full scale TSFs near the perimeter, with low pore pressures and having only recently been inundated should not be assumed at risk of experiencing pre-failure instability?

In our view, it may indeed be the case that there are many examples where entrained air and the quasi-saturated zones exist in TSFs in areas of high stress ratio – the authors are anecdotally aware of sites where compression wave ($V_p$) results below the phreatic surface supports this. Indeed, this could be a contributor to anecdotal evidence that some TSFs remain stable despite, when applying undrained strengths to all zones that are contractive and *perceived* to be fully saturated, the computed FoS indicates that instability should occur. However, it is important to emphasise that we are not arguing against the current state of practice that assumes undrained shearing will mobilise in contractive saturated zones (e.g. ICOLD 2025). Without strong evidence of $S_r <$ 100% (and that such a condition would persist) it would be unsafe, in our view, to rely upon the potential effects of quasi-saturated conditions in the analysis of such structures given the significant risks involved.

Centrifuge tests occur in a relatively short period of time - indeed, it is the ability to simulate field-scale processes faster than they would typically occur in situ that forms one of the great benefits of centrifuge testing. Full scale TSFs are constructed and operated over a period of decades. Given the likely time-dependence of the quasi-saturated region (Holocher et al. 2003) the danger of directly extrapolating centrifuge behaviour to full-scale slopes becomes evident. It is also noteworthy that dynamic geotechnical centrfuge testing commonly adopts stingent measures to achieve saturation (e.g. Kokkali et al. 2018).

The hypothesis of the current paper, and experimental data which appears to support it, points to the need for better characterisation of the quasi-saturated zone in situ. While various techniques are in current use, such as $V_p$, and are emerging (e.g Reid et al. 2023c) it is fair to say that this is an area where significant improvement in the state of practice is possible. Being able to accurately measure $S_r$ in the quasi-saturated zone and above the phreatic surface could lead to more realistic assessments of the risk of TSF slope instability in the future.

## 5 CONCLUSIONS

A series of two beam centrifuge tests on SFS slopes were carried out in an attempt to trigger static liquefaction under a CSD stress path. This was achieved by increasing the phreatic surface through an upstream reservoir while monitoring conditions within the slope. One test used water while another used Methocell with $\sqrt{N}$ viscosity. Both were prepared in a loose condition using MT, resulting in states at which pre-failure instability was seen in laboratory element HCTS tests on a CSD stress path. However, neither slope appears to have exhibited pre-failure instability.

To investigate this behaviour, supplementary CSD element tests were carried out to assess the mechanical behaviour of the sand when under potential poor-quality saturation conditions with significant entrained air. These results suggested that entrained air would significantly reduce the potential for brittle pre-failure instability, generally consistent with other studies on the response of near-saturated loose soils.

Finally, the implications of the centrifuge and experimental tests were outlined. While the potential for entrained air in the quasi-saturated zone to affect the potential for slope instability initiation of real TSFs appears highly likely, significant caution in the application of this observation to the analysis of real TSFs with contractive and brittle tailings is essential. Further efforts to better characterise $S_r$ above and below the phreatic surface would be valuable.

## ACKNOWLEDGEMENTS

This work forms part of TAILLIQ (Tailings Liquefaction), which is an Australian Research Council (ARC) Linkage Project supported by financial and in-kind contributions from Anglo American, BHP, Freeport-McMoRan, Newmont, Rio Tinto, and Teck. We also acknowledge the assistance of NGCF staff in carrying out the experiments.

## REFERENCES

Arroyo, M. and Gens, A. (2021). Computational analyses of Dam I failure at the Corrego de Feijao mine in Brumadinho, CIMNE report to Value.

Coutinho, R.R, et al. 2025. Static liquefaction susceptibility of a Brazilian Iron Ore Tailings Dam. *International Journal of Geomechanics* 25(8).

Fanni, R., Reid, D., and Fourie, A.B. (2022). Effect of principal stress direction on the instability of sand under the constant shear drained stress path. *Géotechnique* 74(9).

Fanni, R., Reid, D., and Fourie, A.B. (2025). Drained and undrained behaviour of a sandy silt gold tailings under general multiaxial conditions. *Géotechnique*, ahead of print.

Faybishenko, B.A. (19950. Hydraulic behavior of quasi-saturated soils in the presence of entrapped air: Laboratory experiments. *Water Resources Research* 31, no. 10: 2421–2435.

Holocher, J., Peeters, F., Aeschbach-Hertig, W., Kinzelbach, W., Kipfer, R. (2003). Kinetic Model of Gas Bubble Dissolution in Groundwater and Its Implications for the Dissolved Gas Composition. Environmental Science and Technology 37(7).

ICMM. (2020). Global industry standard on tailings management.

ICOLD. (2025). Tailings Dam Safety – Bulletin 194. Routledge, Taylor and Francis Group.

Kokkali, P., Abdoun, T. and Zeghal, M. (2018). Physical modelling of soil liquefaction: Overview of LEAP production test at RPI. *Soil Dynamics and Earthquake Engineering* 113: 629-649.

Morgenstern, N.R., Vick, S.G., Viotti, C.B., and Watts, B.D. (2016). Fundão Tailings Dam Review

Ng, C.W.W., Crous, P.A., Jacobsz, S.W. (2023). Centrifuge and numerical modelling of liquefied flow and nonliquefied slide failures of tailings dams. *ASCE Journal of Geotechnical and Geoenvironmental Engineering* 149(9).

Olson, S.M., Stark, T.D., WW, H., and Castro, G. (2000). 1907 Static liquefaction flow failure of the North Dike of Wachusett Dam. Journal of Geotechnical and Geoenvironmental Engineering, 126: 1184–1193. doi:10.1061/(ASCE)1090-0241(2000)126:12(1184).

Reid, D. and Fourie, A. (2019). A direct simple shear device for static liquefaction triggering under constant shear drained loading. *Géotechnique Letters*, 9: 142–146. doi:10.1680/jgele.19.00011.

Reid, D. and Fourie, A. (2024). Development and outcomes of a tailings slope stability comparative design exercise. Canadian Geotechnical Journal 61(8).

Reid, D., Dickinson, S., Mital, U., Fanni, R., and Fourie, A. (2021). On some uncertainties related to static liquefaction triggering assessments. *Proceedings of the Institution of Civil Engineers——Geotechnical Engineering*, 175(2): 181–199. doi:10.1680/jgeen.21.00054.

Reid, D., Fanni, R., and Fourie, A. (2023a). Is the maximum shear stress, in an assumed constant shear drained stress path, really constant? 10th European Conference on Numerical Methods in Geotechnical Engineering (NUMGE2023)

Reid, D., Urbina, F., Tiwari, B. Fanni, R., Smith, K. and Fourie, AB. (2023b). Effect of saturation confining pressure on accessible density and shear behaviour of a sandy silt tailings. *Geotechnique Letters* 13 (2).

Reid, D., Fourie, A., Fridjonsson, E., Jervis-Bardy, N., Reyes, M. and Nuriakhmetov. (2023c). Potential Application of Nuclear Magnetic Resonance to Infer In Situ Degree of Saturation in Tailings. *ASCE Journal of Geotechnical and Geoenvironmental Engineering* 149(5).

Reid, D., Fanni, R., and Fourie, A. (2024). A new method for producing uniform, loose, initially unsaturated specimens. *Geotechnique Letters* 14(4).

Robertson, P.K., de Melo, L., Williams, D.J. and Wilson, G.W. (2019). Report on the expert panel on the technical causes of the failure of Feijao Dam I.

Sasitharan, S., Robertson, P.K., Sego, D.C. and Morgenstern, N.R. (1993). Collapse behaviour of sand. *Canadian Geotechnical Journal* 30(4).

Skopek, P., Morgenstern, N.R., Robertson, P.K. and Sego, D. (1994). Collapse of dry sand. Canadian Geotechnical Journal 31(6).

Souza, A., Telles, A., Reid, D., Fourie, A., Almeida, M. (2024). Instability of sand under a lateral extrusion stress path with different drainage conditions. *Soils and Foundations* 64(6).

Take, W.A., Bolton, M.D., Wong, P.C.P. and Yeung, F.K. (2004). Evaluation of landslide triggering mechanisms in model fill slopes. *Landslides* 1:173-184.

Take, W.A., Beddoe, R.A. (2014). Base liquefaction: a mechanism for shear-induced failure of loose granular slopes. *Canadian Geotechnical Journal* 51.

Urbina, F., Fourie, A.B., and Reid, D. (2025). Experimental program for the determination of the saturation threshold for brittle behaviour in loose sandy silt gold tailings. *ASCE J. of Geo. and Geoen. Eng* .– Ahead of print.

Wang, Y., Vo, T. and Russell, A.R. 2024. Modelling unsaturated silty tailings and the conditions required for static liquefaction. Geotechnique 24(12).

Zhang, W., and Askarinejad, A. (2019). Centrifuge modelling of submarine landslides due to static liquefaction. *Landslides* 2019 16:1921–1938

Zhang, W., and Askarinejad, A. (2020). Centrifuge modelling of static liquefaction in submarine slopes: scaling law dilemma. *Canadian Geotechnical Journal*, 58: 200–209. doi:10.1139/cgj-2019-0417.

Zhu, F., Zhang, W. and Puzrin, A.M. (2024). The slip surface mechanism of delayed failure of the Brumadinho tailings dam in 2019. *Nature Communications Earth & Environment* 5(1)